# Optimal-Sampling-inspired Self-Triggered Control

Manel Velasco, Pau Martí
Department of Automatic Control
Universitat Politècnica de Catalunya
manel.velasco@upc.edu,pau.marti@upc.edu

Enrico Bini
Scuola Superiore Sant'Anna
Pisa, Italy
enrico.bini@sssup.it

***Abstract*—Self-triggered control is an appealing sampling strategy that promises to preserve the same control performance as traditional (periodic) sampling, yet consuming less computing resource by executing the controller less frequently. While the stability of self-triggered controllers is often addressed, their capacity to actually reduce the cost is more difficult to be evaluated.**

**Inspired by a recent result on the optimal density of the sampling instants that minimizes the control cost, in this paper we propose a new self-triggered control strategy. The proposed sampling rule is extremely simple and effective. Significant cost reductions compared to the optimal periodic controller are shown even with larger minimum intersample separation. Thanks to the simplicity of the sampling rule, we also implemented the proposed self-triggered controller over a physical plant. The experimental results are aligned with the theoretical ones.**

## I. Introduction

In digital control systems, controllers are implemented over computing devices. Controllers sample, compute the control action, and actuate in loop during the entire lifetime of the plant. In classic sampled-time control theory, these operations are performed periodically, that is, the time interval between two consecutive samples is set to a constant less than a maximum allowable sampling period, e.g. [13].

In event-driven sampling the periodic sampling hypothesis is relaxed. It is permitted to design novel sampling rules based on different paradigms related to the utilization of computing resources and the desired control performance.

To best of our knowledge, the majority of the existing literature focuses on showing that event-driven sampling reduces the amount of used resources (network, processor time, battery) compared to the traditional periodic implementation, while guaranteeing given control performance properties. See, for example, the classical study in [17], latest results such as [4] and [14], or a recent overview in [7].

However, it is infrequent to find event-driven control approaches targeting the design of optimal sampling rules. To the best of our knowledge, the problem of determining the optimal event rule, in the sense of minimizing the control cost with the same (or less) resource consumption, has not yet got a final answer. Several attempts in this direction do exist, see e.g., [15], [10], [11] or [12]. Their contribution rely on the fact that they offer feasible formulations for the optimal event rule under different settings while identifying possible limitations in terms of computational tractability or practical implementation. Therefore, further research is justified to overcome these limitations.

Additionally, there exist approaches spanning between periodic and event-driven sampling, in which optimal sampling was addressed [16], [2], [5] or [8]. Although not being strictly event-driven approaches, they could be used for comparative evaluation of new sampling proposals.

The closest results in the direction of designing optimal event rules in terms of minimizing control cost and possibly resource utilization can be found in [18] and [6]. Both approaches are based on maximizing the time until the next control update is needed to preserve stability or to minimize the control cost. In [18] the maximization is formulated in the continuous LQR formalism, and considering that the rest of the (future) controller executions will be according to standard periodic time-triggered updates. In [6] the maximization is formulated in the discrete LQR formalism, and it is performed without taking into account the influence of future updates. In addition, [6] provides a tunable triggering mechanism that allows trading off control performance and resource utilization. Finally, in [3] it is investigated the optimal sampling sequence made of a finite number of samples over a finite time horizon. An optimality condition is formulated for first order systems. Such a condition, reported later in Lemma 1, has significantly inspired this paper.

*Contribution of the paper:* In this paper, we present a novel sampling rule for event-based controllers inspired in the optimal sampling patterns proposed by Bini and Buttazzo [3], which was proved to be optimal for first-order systems and large number of sampling instants over the given finite horizon (Section III). The proposed sampling rule is proved to be stable (Section IV). Some design guidelines are also given in Section V. Thanks to the simplicity of the sampling rule, we were able to quickly and simply implement the proposed controller over a physical plant, as described in Section VI. Finally, in Section VII we compare our proposed sampling method with other existing ones, under various settings.

## II. Background

We consider a linear system governed by

$$\begin{cases} \dot{x} = Ax + B\bar{u} \\ x(0) = x_0, \end{cases} \tag{1}$$

where $x \in \mathbb{R}^n$ and $\bar{u} \in \mathbb{R}^m$ are the state and input signals, and $A \in \mathbb{R}^{n\times n}$ are $B \in \mathbb{R}^{n\times m}$ are matrices describing the system dynamics.

The control input signal $\bar{u}$ is constrained to be piecewise constant:

$$\bar{u}(t) = u_k \qquad \forall t \in [t_{k-1}, t_k),$$

with

$$\mathcal{T} = \{t_k \in \mathbb{R} \ : \ k = 0, \dots, N,\, t_0 = 0,\, t_N = T,\, t_{k+1} > t_k\} \tag{2}$$

being the set of *sampling instants* over the finite time horizon of length $T$. Often, we represent a sampling pattern by the values that separates two consecutive instants that are called *sampling intervals* $\tau_k$. The sampling instants and the sampling intervals are related to one another through to the relations

$$\begin{cases} t_0 = 0 \\ t_k = \sum_{i=0}^{k-1} \tau_i \quad k \geq 1, \end{cases} \qquad \tau_k = t_{k+1} - t_k.$$

In periodic sampling we have $\tau_k = \tau$ for all $k$, with $\tau = T/N$ the period of the sampling. Through usual time discretization techniques, by setting

$$\Phi(\tau) = e^{A\tau}, \qquad \bar{A}_k = \Phi(\tau_k), \tag{3}$$

$$\Gamma(\tau) = \int_0^\tau e^{A(\tau - t)}\, dt\, B, \qquad \bar{B}_k = \Gamma(\tau_k), \tag{4}$$

the dynamics (1) can be equivalently described by the following discrete-time time-varying system

$$\begin{cases} x_{k+1} = \bar{A}_k x_k + \bar{B}_k u_k \\ \text{given } x_0 \end{cases} \tag{5}$$

with $x_k = x(t_k)$ for all $t_k \in \mathcal{T}$ being the state sampled at $t_k$.

The optimal finite-horizon LQR problem is about finding the input signal which minimizes the cost

$$J = \int_0^T (x'Qx + \bar{u}'R\bar{u})\, dt + x(T)'Sx(T) \tag{6}$$

with $Q, S \in \mathbb{R}^{n \times n}$ positive semi-definite and $R \in \mathbb{R}^{m \times m}$ positive definite matrices (to denote the transpose of any matrix $M$ we use the compact Matlab-like notation $M'$).

Although to best of our knowledge the problem of finding the optimal set of sampling instants $\mathcal{T}$ minimizing the cost $J$ is still open, recently the problem was solved under some hypothesis [3]. Before, recalling here the main result of [3], which motivates the self-triggered sampling rule proposed in this paper, some additional definitions are needed.

To describe the temporal distribution of the $N$ sampling instants $\mathcal{T}$ over the time interval of length $T$, we define the *sampling density* $\sigma_N : [0, T] \to \mathbb{R}^+$ as

$$\sigma_N(t) = \frac{1}{N\tau_k} \qquad \forall t \in [t_k, t_{k+1}). \tag{7}$$

This expression is a good definition of density for the sampling instants. In fact, for any $k$ and $\ell$ with $0 \leq k \leq \ell \leq N$, we have

$$\begin{aligned} \int_{t_k}^{t_\ell} \sigma_N(t)\, dt &= \sum_{i=k}^{\ell-1} \int_{t_i}^{t_{i+1}} \sigma_N(t)\, dt = \sum_{i=k}^{\ell-1} \int_{t_i}^{t_{i+1}} \frac{1}{N\tau_i}\, dt \\ &= \frac{1}{N} \sum_{i=k}^{\ell-1} \frac{t_{i+1} - t_i}{\tau_i} = \frac{1}{N} \sum_{i=k}^{\ell-1} 1 \\ &= \frac{\ell - k}{N}, \end{aligned} \tag{8}$$

which means that by integrating the density between any two sampling instants we find exactly the number of sampling instants over the interval, relative to the total number $N$. Hence, the sampling density indicates whether the interval is more or less populated by sampling instants. In the special case of $k = 0$ and $\ell = N$, we find the useful normalization property that

$$\int_0^T \sigma_N(t)\, dt = \int_{t_0}^{t_N} \sigma_N(t)\, dt = 1.$$

If any given sampling method generates the set of sampling instants $\mathcal{T}$ for all numbers $N$ of sampling instants over $[0, T]$, we can remove the dependency on $N$ by defining the *asymptotic sampling density* as the following limit

$$\sigma(t) = \lim_{N \to \infty} \sigma_N(t),$$

whenever it exists.

In [3] it is demonstrated a link between the asymptotic sampling density of the optimal sampling instants $\mathcal{T}$ minimizing the cost $J$ of (6), and the optimal continuous-time control input $u^*$. First, as the number of sampling instants $N$ tends to infinity, the optimal sampled-time control input $\bar{u}^*$ tends the optimal continuous-time input $u^*$. Second, the optimal sampling instants of $\mathcal{T}$, that are the points at which $\bar{u}^*$ changes value, are denser when $|\dot{u}^*|$ is high, while they can be less dense when $u^*$ is closer to a constant ($|\dot{u}^*|$ close to zero). This intuition is also summarized by the next result.

*Lemma 1 (Lemma 6 in [3]):* In first-order systems ($n = m = 1$) with weight of the final state $S$ equal to the solution of the continuous ARE (Algebraic Riccati Equation), the asymptotic density of the optimal sampling which minimizes the cost $J$, is

$$\sigma_{\mathsf{opt}} \propto |\dot{u}^*|^{2/3} \tag{9}$$

being $u^*$ the optimal continuous-time input.

Although the exponent of $2/3$ in (9) is difficult to explain intuitively, the intuition of sampling more frequently (with high sampling density) whenever the optimal continuous-time input $u^*$ grows quickly is reasonable. In fact, as $N \to \infty$ the optimal sampled-time input $\bar{u}^*$ is shown to be the discrete-time piecewise constant function that better approximates the continuous-time $u^*$. Sets of sampling instants $\mathcal{T}$ with asymptotic density of (9) showed a remarkable capacity to reduce the cost $J$ even in more general hypothesis that first-order systems. We conjecture then that Lemma 1 is valid also in general, although only numerical evaluation was made [3].

## III. The proposed sampling rule

Our intended goal is to develop a sampling strategy that mimics the sampling density of (9), since this density is guaranteed to be optimal, at least under some hypothesis (first-order system). Translating the theoretical result of Lemma 1 to the real world does however pose some challenges listed below:

1) the sampling density of (7) is defined only over a *known* time horizon $T$, while we would like to develop a sampling rule which may run potentially forever;
2) the link established in (9) is *open-loop*. That is, given the plant and an initial state (1), and given a cost function (6), the optimal continuous-time control signal $u^*$ can be computed. This function $u^*$ can be used to obtain the set of $N$ sampling instants that will be applied in the digital implementation. However, the open-loop nature of this procedure makes it unpractical. Any disturbance may alter the state and, in turn, the optimal continuous-time input $u^*$ needed from the new perturbed state. Such a change in $u^*$, however will not be reflected in the set $\mathcal{T}$ of pre-computed sampling instants. Hence, we aim at designing a sampling rule that can react to state variations, but still mimic the optimal sampling density of (9).

In Section III-A we explain our proposed method to determine the sampling instants according to a given density, while in Section III-B we formulate the proposed sampling rule.

### A. The closed-loop sampling rule

An open-loop sampling method that achieves any asymptotic sampling density $\sigma$ defined over $[0, T]$, is to select the $N$ sampling instants such that

$$\int_{t_k}^{t_{k+1}} \sigma(t)\, dt = \frac{1}{N}, \qquad k = 0, \dots, N-1. \tag{10}$$

Setting the sampling instants according to (10) guarantees an average sampling period of $\frac{T}{N}$ over the interval $[0, T]$. A drawback, however, is that this methods requires to know in advance the time horizon $T$. An equivalent formulation of (10), which can be applied to any sampling density possibly defined over $[0, \infty)$, is to sample such that

$$\int_{t_k}^{t_{k+1}} \sigma(t)\, dt = \eta, \tag{11}$$

with $\eta$ being a given constant. This way we cannot control any longer the average sampling period (which was $\frac{T}{N}$ over the finite horizon $[0, T]$). But still we can control the sampling periods through $\eta$: smaller values of $\eta$ will produce denser sampling instants and vice versa.

Since our goal is to mimic the sampling density $|\dot{u}^*|^{2/3}$, proved optimal for first-order systems (Lemma 1), we set $\sigma(t) = |\dot{u}^*(t)|^{2/3}$ in (11), with $u^*(t)$ being the optimal continuous-time input

$$u^*(t) = Lx(t) = Le^{(A+BL)(t-t_k)}x_k, \tag{12}$$

with $L$ optimal continuous-time feedback gain found by minimizing the cost $J$ of (6) when $T$ tends to $\infty$. Without loss of generality, henceforth we assume $t_k = 0$ in (12) and subsequent equations.

Summarizing, at each sampling instant $t_k$, the next sampling instant $t_{k+1}$ is determined as a function of the system state $x_k$ at $t_k$, by defining the next sampling instant as

$$t_{k+1} = t_k + \tau_k,$$

with $\tau_k$ such that

$$\int_0^{\tau_k} |\dot{u}^*|^\alpha\, dt = \eta, \tag{13}$$

and $u^*(t)$ defined as in (12), $\eta$ controlling the frequency of sampling. We remark that the optimality of the exponent $\alpha = \frac{2}{3}$ was proved only under some restrictive hypothesis (Lemma 1). Hence, we explore more general sampling rules with any exponent $\alpha \geq 0$. Periodic sampling also belongs to this class, by setting $\alpha = 0$.

### B. First-order approximation of the optimal continuous-time input

The sampling rule of (13) poses serious difficulties to a simple implementation. It requires

- to compute the derivative of the optimal continuous-time input $u^*(t)$ of (12) at every sampling instant,
- to raise this function $u^*(t)$ to the power of $\alpha$, compute its absolute value, and
- integrate it until the integral reaches the value of $\eta$, as indicated by the sampling rule (13).

To overcome this difficulty and to be able to efficiently compute the integral, we approximate the optimal $u^*(t)$ with initial state $x_k$ to the first order (higher order approximations will be investigated in further works), that is

$$u^*(t) = Le^{(A+BL)t}x_k \approx L(I + (A+BL)t)x_k. \tag{14}$$

From this approximation, then we also have

$$\dot{u}^*(t) = L(A+BL)e^{(A+BL)t}x_k \approx L(A+BL)x_k,$$

which is a constant over time and can then be simply integrated as in (13)

$$\int_0^{\tau_k} |L(A+BL)x_k|^\alpha\, dt = \eta,$$

and allows us to find the next sampling instant by

$$\tau_k = \frac{\eta}{|L(A+BL)x_k|^\alpha}.$$

This sampling rule, however, has a drawback: when $x_k \in \ker(L(A+BL))$, then $\tau_k$ goes to infinity. In fact, for such a sampling rule it is not even possible to prove stability. To guarantee that the sampling intervals are upper bounded, we add a positive constant $\gamma$ in the integration, so that

$$\tau_k = \frac{\eta}{|L(A+BL)x_k|^\alpha + \gamma}.$$

Equivalently, to highlight the dependency on the maximum sampling interval $\tau_{\mathsf{max}}$ and on $\eta$, which determines how

frequently we want to sample, the same sampling rule can be written as:

$$\tau_k = \tau_{\mathsf{max}} \frac{1}{\frac{\tau_{\mathsf{max}}}{\eta}|L(A+BL)x_k|^\alpha + 1}. \tag{15}$$

As a simple consequence of $|L(A+BL)x_k| \geq 0$, it follows that it is always $\tau_k \leq \tau_{\mathsf{max}}$. In addition, if $|L(A+BL)x_k|$ is upper bounded then the minimum sampling interval $\tau_k$ can be lower bounded. In fact,

$$|L(A+BL)x_k| \leq \beta \;\Rightarrow\; \tau_k \geq \tau_{\mathsf{min}} := \tau_{\mathsf{max}} \frac{1}{\frac{\tau_{\mathsf{max}}}{\eta}\beta^\alpha + 1}. \tag{16}$$

The rule of (15) determines the next sampling interval $\tau_k$ from a given state $x_k$. The control signal applied over $[t_k, t_k + \tau_k)$ is computed via the optimal feedback gain $\bar{L}(\tau_k)$ as computed from the discretized system with period $\tau_k$.

In summary, we propose the control strategy described below:

$$\begin{aligned} \tau_k &= \tau_{\mathsf{max}} \frac{1}{\frac{\tau_{\mathsf{max}}}{\eta}|L(A+BL)x_k|^\alpha + 1} \\ u_k &= \bar{L}(\tau_k)\, x_k \\ x_{k+1} &= \bar{A}_k x_k + \bar{B}_k u_k = \bar{\mathcal{A}}(\tau_k)\, x_k \end{aligned}$$

with $\bar{\mathcal{A}}(\tau_k)$ being the closed loop dynamics with sampling period $\tau_k$.

Finally, we require the system to be stable for $\tau_k = \tau_{\mathsf{max}}$, that is the matrix $\bar{\mathcal{A}}(\tau_{\mathsf{max}})$ is Schur.

## IV. Stability condition

To prove the stability, we aim at finding a *common quadratic Lyapunov function* (CQLF) around the equilibrium point, that is common to all sampling intervals in the interval $[\tau_{\mathsf{min}}, \tau_{\mathsf{max}}]$. The candidate CQLF is $V(x) = x'Px$, the $P$ positive definite matrix solution of the Lyapunov equation

$$\bar{\mathcal{A}}'(\tau_{\mathsf{max}})\, P\, \bar{\mathcal{A}}(\tau_{\mathsf{max}}) - P + Q = 0, \tag{17}$$

with $Q > 0$ being the decrease rate, and $\tau_{\mathsf{max}}$ the maximum sampling period of the sampling rule (15). We know that such a $P$ exists, because the system is stable when $\tau_k = \tau_{\mathsf{max}}$.

Let us define

$$\rho(\tau) = \max\left\{\sigma\big(\bar{\mathcal{A}}'(\tau)\, P\, \bar{\mathcal{A}}(\tau) - P\big)\right\} \tag{18}$$

that is the maximum among the eigenvalues of $\bar{\mathcal{A}}'(\tau)\, P\, \bar{\mathcal{A}}(\tau) - P$, where $\sigma$ denotes the matrix spectrum. Since the matrix is Hermitian, eigenvalues are reals, and the $\rho(\tau)$ is well defined.

The function $\rho(\tau)$ is continuous, since it is the composition of the continuous map $\tau \mapsto \bar{\mathcal{A}}(\tau)$, the continuous map $\bar{\mathcal{A}} \mapsto \bar{\mathcal{A}}' P \bar{\mathcal{A}} - P$, the continuous map of a matrix to its spectrum, and finally the maximum over a finite set (which is also continuous).

At $\tau = \tau_{\mathsf{max}}$, from (17) we have, $\rho(\tau_{\mathsf{max}}) = -\lambda_{\mathsf{min}}(Q) < 0$, that is the opposite of the smallest eigenvalue of $Q$. Because of the continuity of $\rho(\tau)$ at $\tau_{\mathsf{max}}$, we have

$$\forall \epsilon > 0,\ \exists \delta > 0,\ \forall \tau, |\tau - \tau_{\mathsf{max}}| < \delta, \quad |\rho(\tau) - \rho(\tau_{\mathsf{max}})| < \epsilon.$$

By setting $\epsilon = \lambda_{\mathsf{min}}(Q) > 0$, we have then

$$\exists \delta > 0,\ \forall \tau, |\tau - \tau_{\mathsf{max}}| < \delta, \quad -2\lambda_{\mathsf{min}}(Q) < \rho(\tau) < 0.$$

For convenience, we select a closed interval $[\tau_{\mathsf{min}}, \tau_{\mathsf{max}}]$ within the neighborhood of $\tau_{\mathsf{max}}$ with radius $\delta$, so that

$$\forall \tau \in [\tau_{\mathsf{min}}, \tau_{\mathsf{max}}], \quad \rho(\tau) < 0$$

We claim that $V(x) = x'Px$ is a CQLF, for all $x_k$ such that the corresponding sampling interval $\tau_k$ belongs to $[\tau_{\mathsf{min}}, \tau_{\mathsf{max}}]$. In fact, let us pick $x_k$ such that

$$x_k \neq 0, \quad |L(A+BL)x_k| \leq \sqrt[\alpha]{\eta\left(\frac{1}{\tau_{\mathsf{min}}} - \frac{1}{\tau_{\mathsf{max}}}\right)}$$

For such $x_k$, we are certain that the corresponding $\tau_k$ belongs to the interval $[\tau_{\mathsf{min}}, \tau_{\mathsf{max}}]$. Then, we have

$$\begin{aligned} V(x_{k+1}) - V(x_k) &= x_k'(\bar{\mathcal{A}}'(\tau_k) P \bar{\mathcal{A}}(\tau_k) - P)x_k \\ &\leq \rho(\tau_k)\|x_k\|^2 \\ &< 0. \end{aligned}$$

We have then found a neighborhood of the equilibrium point 0, in which the Lyapunov function $V(x_k) = x_k' P x$ decreases along trajectories.

## V. Controller design

The sampling rule defined in (15) depends on several parameters (the exponent $\alpha$, the maximum sampling period $\tau_{\mathsf{max}}$, and the control of the density $\eta$) that permit to tune our proposed controller. To illustrate the design procedure, the following example will be used, where the considered plant (1) is a double integrator circuit with

$$A = \begin{bmatrix} 0 & -23.8 \\ 0 & 0 \end{bmatrix}, \qquad B = \begin{bmatrix} 0 \\ -23.8 \end{bmatrix}, \qquad x_0 = \begin{bmatrix} 1 \\ 1 \end{bmatrix}$$

and where the cost (6) is characterized by the weighting matrices

$$Q = \frac{1}{23.8^2}\, I, \qquad R = \frac{2}{23.8}, \qquad S = 10^{-4}\begin{bmatrix} 3 & -5 \\ -5 & 20 \end{bmatrix}.$$

The values are chosen to have smooth plots, later shown in Figures 1, 2, 3, and 4. Clearly, the design procedure does not change for different values.

The sampling rule (15) is characterized by several design parameters. First of all, the weighting matrices $Q$, $R$ and $S$ of the cost function (6) are the standard control settings to be specified in order to obtain the optimal continuous-time gain $L$.

In addition, the rule provides more settings that permit characterizing the temporal behavior of the triggering events. In fact, looking at the rule, it could be assumed that the two main parameters are $\eta$ that permits to control the frequency of sampling, and $\alpha$, that with a setting of $\alpha = 2/3$ was shown to be optimal for first order systems. However, designing only with these parameters could lead to unfeasible implementation requirements. For example, by simply specifying a big $\eta$, that is, willing a low frequency sampling (in average) to release

| $\tau_{\mathsf{max}}$ | $\tau_{\mathsf{min}}$ | $\alpha$ | $\eta$ | $N$ | $\min\{\tau_k\}$ | $\max\{\tau_k\}$ | $\tau_{\mathsf{avg}} = \frac{t_N}{N}$ | $\frac{J-J_\infty}{J_\infty}$ $(\times 10^{-5})$ |
|---|---|---|---|---|---|---|---|---|
| 38 | 2 | 0.7 | 0.0101 | 71 | 5.1 | 30.9 | 13. 8 | 14.35 |
| 38 | 8.2 | 0.7 | 0.0499 | 35 | 16.6 | 36.2 | 27.9 | 130.00 |
| 38 | 19.5 | 0.1 | 0.0501 | 42 | 20.9 | 26.0 | 23.7 | 170.00 |
| 38 | 5 | 0 | 0.0058 | 194 | 5 | 5 | 5 | 9.82 |
| 38 | 5 | 0.2 | 0.0090 | 93 | 6.9 | 15.5 | 10.7 | 1.98 |
| 38 | 5 | 0.4 | 0.0141 | 63 | 8.2 | 27.6 | 15.8 | 0.30 |
| 38 | 5 | 0.6 | 0.0220 | 47 | 10.2 | 33.9 | 20.9 | 0.50 |
| 38 | 5 | 0.8 | 0.0344 | 39 | 12. 6 | 36.5 | 25.1 | 0.78 |
| 38 | 5 | 1 | 0.0537 | 35 | 15.2 | 37.3 | 28.5 | 1.2 |

TABLE I
EXPLORING THE CONTROLLER DESIGN PARAMETERS (ALL TIMES ARE IN MILLISECONDS).

computing power to other tasks could lead to too long sampling intervals that may violate fundamental sampling rules such as the Nyquist-Shannon sampling theorem or standard rules of thumb for selecting sampling periods. Or on the contrary, specifying a small $\eta$, that is, willing a high frequency sampling to improve performance could lead to too short sampling intervals that may be impossible to serve by the computing platform.

Therefore, like in the case of LQR design, additional constraints must be considered for the design of the sampling rule. The design procedure of our event-driven controller is summarized below:

1) Compute the optimal control feedback gain $L$ of the continuous-time system.
2) Select a value $\tau_{\mathsf{max}}$, such that the discrete-time closed loop dynamics $\bar{A}(\tau_{\mathsf{max}})$ is stable. A standard rule of thumb [1] indicates that the number of samples per rise time should be $4$ to $10$. Note that the selection of the weighting matrices for LQR design will determine the location of the continuous-time closed loop poles. And they will impose a closed loop dynamics that is characterized for example by the rise time (among many other parameters). Sampled-data systems theory advises that for a discrete-time controller implementation the sampling period should be chosen such that between 4 and 10 samples will be taken during this rise time.
3) Determine the entire state space $\mathcal{X}$ from the physical constraint of the plant, and then compute
$$\beta := \sup_{x \in \mathcal{X}} |L(A+BL)x|. \tag{19}$$
4) From the characteristics of the computing platform, we find the minimum feasible value $\tau_{\mathsf{mim}}$ of the sampling period. If $\tau_{\mathsf{min}} > \tau_{\mathsf{max}}$, then no controller can satisfy the constraints. Otherwise, if all sampling periods are required to be not smaller than $\tau_{\mathsf{min}}$, from (16) it follows that
$$\tau_k = \tau_{\mathsf{max}} \frac{1}{\frac{\tau_{\mathsf{max}}}{\eta}|L(A+BL)x_k|^\alpha + 1} \geq \tau_{\mathsf{max}} \frac{1}{\frac{\tau_{\mathsf{max}}}{\eta}\beta^\alpha + 1} \geq \tau_{\mathsf{min}},$$
from which the following condition on the controller parameters follows
$$\frac{\beta^\alpha}{\eta} \leq \frac{1}{\tau_{\mathsf{min}}} - \frac{1}{\tau_{\mathsf{max}}}. \tag{20}$$
Any controller parameters satisfying (20), with $\beta$ defined as in (19) guarantees that all sampling periods will be in the range $[\tau_{\mathsf{min}}, \tau_{\mathsf{max}}]$.

Let us now follow all these steps for the the example illustrated at the begin of the section.

1) By solving the optimal continuous-time LQR problem, we find $L = \begin{bmatrix} -0.14 & 0.56 \end{bmatrix}$.
2) Considering the continuous-time closed loop poles $s_{1,2} = -6.64 \pm 6.17i$, a suitable choice is $\tau_{\mathsf{max}} = 38\,\mathsf{ms}$.
3) We assume that the state space is $\mathcal{X} = [-1.6, 1.6] \times [-1.6, 1.6]$. Hence, the corresponding upper bound $\beta$ of (19) is $\beta = 9.4$.
4) About the minimum separation, in our example, we assume $\tau_{\mathsf{min}} = 5\,\mathsf{ms}$.

In Table I we explore the design space of the controller of this example. In the table, all times are in milliseconds. The first four columns are the design parameters of the controller: the maximum and minimum sampling periods $\tau_{\mathsf{max}}$ and $\tau_{\mathsf{min}}$ specified at design time, the exponent $\alpha$ in the sampling rule (remember: when $\alpha \to 0$ the sampling tends to be periodic), and the threshold $\eta$. In the last five columns we report the output of the controller over the simulation time interval of one second: the number $N$ of sampling instants, the minimum and maximum sampling period experienced in the simulation, the average sampling period $\tau_{\mathsf{avg}} = \frac{t_N}{N}$, and finally the cost increase relative to the continuous-time optimal cost that in this example is $J_\infty = 0.0012$.

Table I is divided into two sets of rows. The first three emphasize the effect of $\alpha$ and $\eta$ on the timing aspects of the generated sampling pattern. The trajectory over the state space and the sampling patterns of the dynamics generated by the controllers with parameters corresponding to the first three rows are reported in Figures 1, 3 and 4 respectively.

As it can be noticed, for a fixed value of $\alpha = 0.7$ (Figures 1 and 3), the smaller $\eta$, the denser is the sampling and more disperse are the sampling intervals. For a fixed value of $\eta = 0.05$ (Figures 3 and 4), the smaller the $\alpha$, the less disperse are the sampling intervals. In fact, for small $\alpha$ the sampling

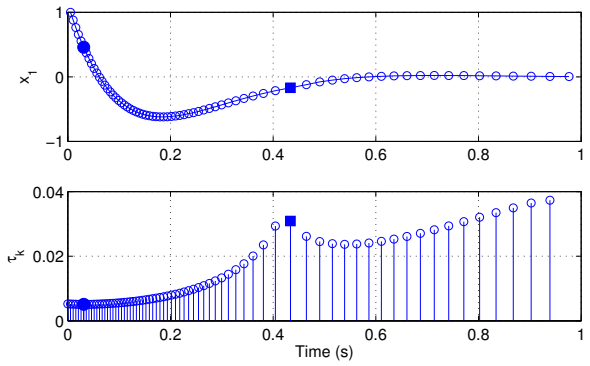


Fig. 1. System response and sampling intervals for $\eta = 0.01$ and $\alpha = 0.7$

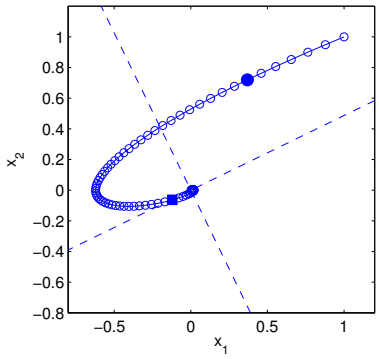


Fig. 2. System response and sampling intervals in the phase portrait for $\eta = 0.01$ and $\alpha = 0.7$

tends to the periodic case. We also remark that the peak in the sampling period, marked with a square in Figure 1 at time $t = 0.43$s, occurs when the state is closer to the kernel of the $L(A + BL)$ represented by an dashed line in the state space of the same dynamics plotted in the phase portrait shown in Figure 2. The shortest sampling interval, marked by a solid dot, occurs when the system state is as far as possible from the $\ker(L(A + BL))$

It is worth noting that the six bottom rows of Table I aim at illustrating the effect of the $\alpha$ and $\eta$ on the timing as well as on the performance. First of all, the relation between $\alpha$ and $\eta$ obeys Eq. (20). Given a fixed $\tau_{\mathsf{max}}$ and $\tau_{\mathsf{min}}$, given a fixed the upper bound $\beta = 9.4$ of the state space $\mathcal{X}$ (19), and giving values to $\alpha = 0, 0.2, 04, 0.6, 0.8, 1$, we obtain different values for $\eta$. And for each $(\tau_{\mathsf{max}}, \alpha, \eta)$ setting, by applying the execution rule (15) we obtain the values reported in the table. It can be noticed that as $\eta$ increases, less samples are taken, and the average sampling interval $\tau_{\mathsf{avg}}$ increases. The last column is the cost achieved by the method. We observe that the cost is always lower than the periodic case ($\alpha = 0$), although having an even larger minimum sampling interval (column "$\min\{\tau_k\}$). This confirms the effectiveness of the proposed sampling rule.

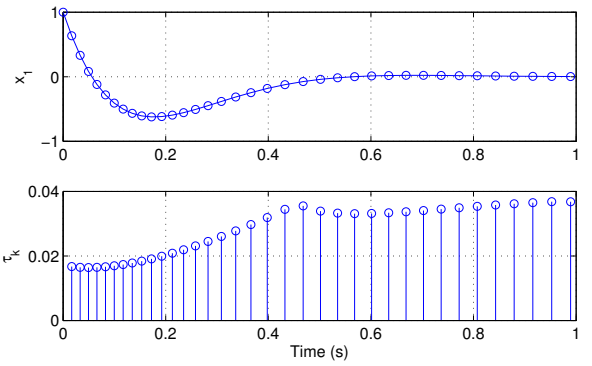


Fig. 3. System response and sampling intervals for $\eta = 0.05$ and $\alpha = 0.7$

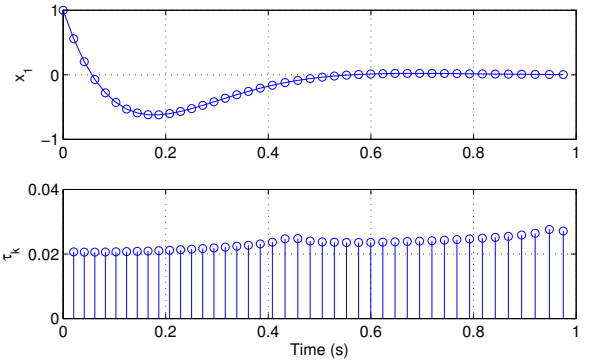


Fig. 4. System response and sampling intervals for $\eta = 0.05$ and $\alpha = 0.1$

## VI. Implementation

The simplicity of the sampling rule (15) permits an easy implementation of the proposed self-triggered controllers. The implementation setup consists of the plant to be controlled and the processing platform (hardware and real-time kernel). The plant is a double integrator electronic circuit whose linear continuous-time state-space model (1) is characterized by the $A$ and $B$ matrices given in Section V. The processing platform is Full Flex board equipped with a Microchip dsPIC33FJ256MC710a, running the Erika real-time kernel. The goal of the controller is to make the circuit output voltage to track a given reference signal by applying the appropriate voltage levels to the plant input. See [9] and references therein for further details on the plant, board, and real-time kernel.

The implementation has considered three tasks: a reference signal generator, the self-triggered controller, and a monitoring task. The first one is responsible for generating the reference signal to be tracked. The last one is in charge of sending closed-loop system information such as states' values and timing values to assess the operation of the controller.

The self-triggered controller performs two basic functions. First, it computes the next activation time according to the sampling rule (15), thus obtaining $\tau_k$, and it uses this value to set an alarm that will activate again the controller at the computed next sampling instant. Second, considering the reference signal value (set-point) and the plant state variables

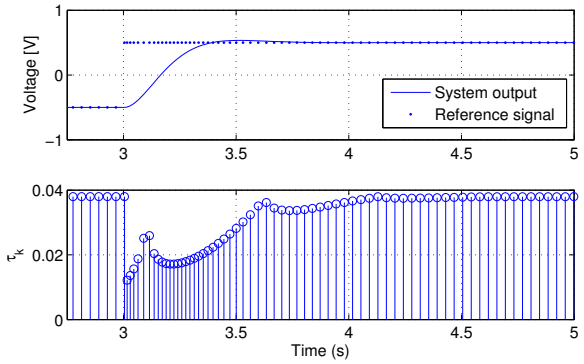


Fig. 5. Step change simulation results

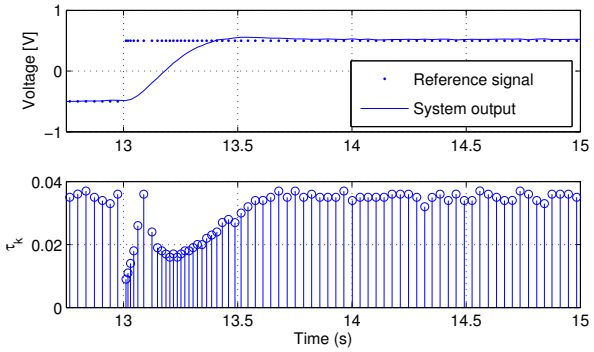


Fig. 6. Step change implementation results

read (sampled) through the dsPIC33 ADC, it calculates the control signal $u_k$ using the controller gain $\bar{L}(\tau_k)$, which is then applied to the plant through the PWM by adequately setting its duty cycle.

As indicated in section III-B, at each controller execution at instant $t_k$, the optimal LQR gain $\bar{L}(\tau_k)$ must be used as feedback gain. This means that the gain changes at each controller execution. To avoid an expensive computation of the optimal LQR feedback gain, which requires the discretization of the system dynamics and the solution of a DARE, we pre-computed and stored in a look-up table the optimal gains to be applied.

The design parameters are the same described in the controller design Section V. The discrete LQR controller gains $\bar{L}(\tau_k)$ are computed for $5 \leq \tau_k \leq 38$ ms (with a 1 ms granularity) using the given $Q$, $R$ and $S$ weighting matrices. In addition, considering the given space $\mathcal{X}$, we took $\alpha = 0.66$, $\eta = 0.0277$. Note that these settings are in accordance to those studied in Table I.

Figure 5 and Figure 6 shows the simulated and experimental step response of the plant, respectively. The main difference between the simulation and the experiment is the presence of noise in the plant measures. In the simulation, no noise is considered. In the experiment, the plant readings have noise, which introduces small variations in the sampled states and then in the calculated activation time with (15). The reduction in the sampling intervals compared to those in the simulation may be caused by the presence of noise in steady state. This would be a good sign because it would mean that the sampling rule is sensitive to noise. The impact of noise on the proposed self-triggered controllers will be further investigated in future work.

## VII. Evaluation

The main motivation of self-triggered control is in the capacity to reduce the cost more aggressively than periodic controllers, with the same or less amount of consumed computing resource. This section further explores the performance of the proposed sampling rule of (15) and compares it with the periodic case.

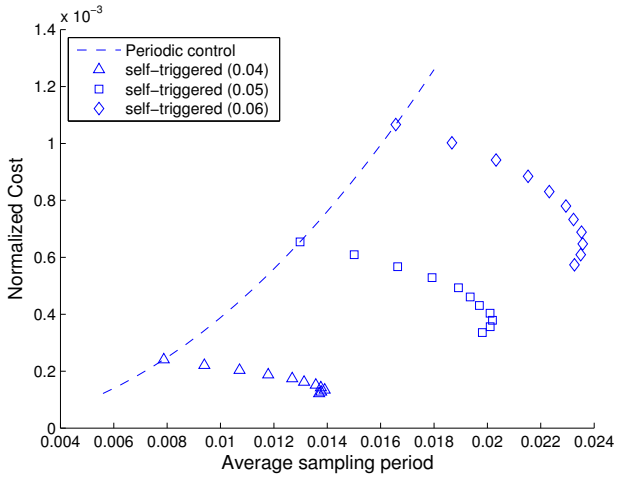


Fig. 7. Execution cost for different values of $\eta$ and $\alpha$, $\eta \in \{0.4, 0.5, 0.6\}$, $\alpha \in \{0, 0.1, \ldots, 1\}$

The control cost in the comparative analysis presented next is computed with the normalized cost defined as

$$c = \frac{J_N - J_\infty}{J_\infty} \tag{21}$$

where $J_\infty$ is the minimal cost of the continuous-time systems, and $J_N$ is the discrete cost corresponding to (6) but with variable sampling intervals, and for $N$ steps.

The main evaluation is presented in Figure 7, where we plot the normalized cost $c$ of (21) over the average sampling intervals $\tau_{\mathsf{avg}}$, defined as

$$\tau_{\mathsf{avg}} = \frac{\sum_{k=0}^{N-1} \tau_k}{N},$$

for the design settings presented in the controller design Section V. The number $N$ of steps in the simulation is determined by the condition on the system state

$$\|x_N\| \leq 10^{-3},$$

which ensures the system output to be close enough to the equilibrium point. In fact, since the system is stabilized, the sampling interval tends to $\tau_{\mathsf{max}}$. Hence, by extending the

simulation time, we would draw wrong conclusions on $\tau_{\mathsf{avg}}$. We underline that average sampling interval is a good metric to measure the goodness or quality of varying sampling rates [6].

The figure shows four curves, one with a parabola shape (dashed line) and the rest plotted with markers (triangle, square or diamond). The dashed line corresponds to the cost obtained by periodic discrete LQR control for different sampling periods. As it can be observed, as the sampling period increases, the periodic controller achieves a greater cost, i.e., it performs worse.

The curves with markers correspond to self-triggered controllers. In fact, each curve corresponds to controllers characterized by different $\eta$ values, $0.04$, $0.05$ and $0.06$. Reminding that $\eta$ indicates the granularity of the space discretization, it can be observed that for small values, e.g., $\eta = 0.4$ (triangles), the average sampling intervals are shorter, and lower costs are achieved.

The shape of each self-triggered curve is found by varying $\alpha = 0, 0.1, 0.2, \ldots, 1$. Recall that $\alpha = 0$ is the case of periodic sampling (top marker for each curve). Observe that as $\alpha$ increases, the average sampling period increases and the cost is reduced! This is an counter-intuitive but very positive behavior: using less computing resources (in average) we obtain a smaller control cost. At some point however, this tendency changes, and as $\alpha$ continue increasing, the average sampling interval starts to decrease and the cost is further reduced. This is more intuitive, in the sense that using more computing resources, lower cost is achieved.

Finally, we observe that the shapes of Figure 7 are in accordance to study presented by Bini and Buttazzo [3]. That is, for each curve, the best marker corresponds to an $\alpha$ value close to $2/3$, setting that was proved to provide the optimal sequence for first order systems.

More in general, the main lesson learned form this simulation study and illustrated in this figure is that self-triggered controllers perform better than the periodic ones while using less resources.

## VIII. Conclusions and future works

In this paper we attempted to translate into practical settings the theoretical result on the optimal asymptotic sampling density for first-order systems [3]. Still, there is space for further improvements.

The implemented sampling rule (15) is based on several approximations that permit to turn the theoretical rule (11) into a practical one. Hence, further analysis is required on what is lost in the approximation, and on using alternative (approximation) approaches. In addition, the parameter that constraints the state space that is heuristically specified could be found through an invariance set analysis. Also, a comparative analysis with the results presented in [6] could help understanding pros and cons of the presented sampling rule. An interesting point is that from a design perspective, the presented rule starts from a design constraint given by $\tau_{\mathsf{max}}$, and then sampling intervals are guaranteed to be $\tau_k \leq \tau_{\mathsf{max}}$. The approach proposed in [6] works in the other direction. From a constraint given by $\tau_{\mathsf{min}}$, sampling intervals are maximized as much as possible, always having $\tau_k \geq \tau_{\mathsf{min}}$. Therefore, the space is explored using two opposite strategies that should meet at some point.

## Acknowledgment

This paper has been partially supported by the Spanish Ministry of Economy and Competitiveness under grants DPI2010-18601 and TEC2013-46938-R

## References

[1] Karl Johan Åström and Björn Wittenmark. *Computer-Controlled Systems. Theory and Design*. Prentice Hall, third edition, 1997.

[2] M.-M. Ben Gaid, A. Çela, and Y. Hamam. Optimal real-time scheduling of control tasks with state feedback resource allocation. *IEEE Transactions on Control Systems Technology*, 2009.

[3] Enrico Bini and Giuseppe M. Buttazzo. The optimal sampling pattern for linear control systems. *IEEE Transactions on Automatic Control*, 59(1):78–90, January 2014.

[4] D.P. Borgers and W.P.M.H. Heemels. Event-separation properties of event-triggered control systems. *Automatic Control, IEEE Transactions on*, 59(10):2644–2656, Oct 2014.

[5] A. Cervin, M. Velasco, P. Marti, and A. Camacho. Optimal online sampling period assignment: Theory and experiments. *Control Systems Technology, IEEE Transactions on*, 19(4):902–910, July 2011.

[6] Tom Gommans, Duarte Antunes, Tijs Donkers, Paulo Tabuada, and Maurice Heemels. Self-triggered linear quadratic control. *Automatica*, 50(4):1279 – 1287, 2014.

[7] W.P.M.H. Heemels, K.H. Johansson, and P. Tabuada. An introduction to event-triggered and self-triggered control. In *Decision and Control (CDC), 2012 IEEE 51st Annual Conference on*, pages 3270–3285, Dec 2012.

[8] Xu-Guang Li, A. Cela, S.-I. Niculescu, and Shi-Guang Wen. Optimization for networked control systems under the hyper-sampling period. In *Control Conference (ECC), 2014 European*, pages 2868–2873, June 2014.

[9] Camilo Lozoya, Pau Martí, Manel Velasco, Josep M. Fuertes, and Enric X. Martin. Resource and performance trade-offs in real-time embedded control systems. *Real-Time Systems*, 49(3):267–307, 2013.

[10] Pau Martí, Manel Velasco, and Enrico Bini. The optimal boundary and regulator design problem for event-driven controllers. In Rupak Majumdar and Paulo Tabuada, editors, *Hybrid Systems: Computation and Control*, volume 5469 of *Lecture Notes in Computer Science*, pages 441–444. Springer Berlin Heidelberg, 2009.

[11] Xiangyu Meng and Tongwen Chen. Optimal sampling and performance comparison of periodic and event based impulse control. *Automatic Control, IEEE Transactions on*, 57(12):3252–3259, Dec 2012.

[12] A. Molin and S. Hirche. On the optimality of certainty equivalence for event-triggered control systems. *Automatic Control, IEEE Transactions on*, 58(2):470–474, Feb 2013.

[13] D. Nesic, A.R. Teel, and D. Carnevale. Explicit computation of the sampling period in emulation of controllers for nonlinear sampled-data systems. *Automatic Control, IEEE Transactions on*, 54(3):619–624, March 2009.

[14] R. Postoyan, P. Tabuada, D. Nesic, and A. Anta. A framework for the event-triggered stabilization of nonlinear systems. *Automatic Control, IEEE Transactions on*, PP(99):1–1, 2014.

[15] M. Rabi, K.H. Johansson, and M. Johansson. Optimal stopping for event-triggered sensing and actuation. In *Decision and Control, 2008. CDC 2008. 47th IEEE Conference on*, pages 3607–3612, Dec 2008.

[16] H. Rehbinder and M. Sanfridson. Integration of off-line scheduling and optimal control. In *Real-Time Systems, 2000. Euromicro RTS 2000. 12th Euromicro Conference on*, pages 137–143, 2000.

[17] Karl Johan Åström and Bo Bernhardsson. Comparison of periodic and event based sampling for first order stochastic systems. In *Proceedings of the 14th IFAC World Congress*, 1999.

[18] M. Velasco, P. Marti, J. Yepez, F.J. Ruiz, J.M. Fuertes, and E. Bini. Qualitative analysis of a one-step finite-horizon boundary for event-driven controllers. In *Decision and Control and European Control Conference (CDC-ECC), 2011 50th IEEE Conference on*, pages 1662–1667, Dec 2011.